Journal of Social Research
P-ISSN: 2827-9832
E-ISSN: 2828-335x
http://ijsr.internationaljournallabs.com/index.php/ijsr

EVALUATION OF THE STRENGTH OF R60 TYPE RAILS AGAINST LOADING HIGH-SPEED TRAINS

Septa Ade Dermawan[1*], Nunung Widyaningsih[2]
Faculty of Engineering Universitas Mercu Buana Jakarta, Indonesia
41121120108@student.mercubuana.ac.id, nunung_widyaningsih@mercubuana.ac.id

ABSTRACT

Currently, Indonesia has entered a new phase in the development of modern transportation infrastructure, namely high-speed trains initiated by PT Kereta Cepat Indonesia China. The design of the facility operated is an Electrical Multiple Unit (EMU) CR400AF that can drive up to speeds of 350 km / h. Of course, high train speed requires the reliability of railway road infrastructure, including the geometry and components of rail roads. The technical specifications of high-speed rail roads have been regulated in the Minister of Transportation Regulation Number 7 of 2022. The type of rail used by high-speed railway line components with a rail road width of 1435 mm is type R60 rail. However, the determination of the type of high-speed railway in Indonesia has not been completed by analyzing the strength of the rail structure in bearing the load working on it. Thus, this study discusses the influence of rail road geometry on the speed of facilities and evaluates the strength of Type R60 rail structures in receiving high-speed train loads. The analysis method uses the Beam on Elastic Foundation (BOEF) method which assumes the behavior of rails as continuous beams that receive loads on elastic foundation pedestals. The results of the study found that the value of the realized radius and minimum radius of the horizontal arch respectively amounted to 9,500 m and 8,502.94 m greater than the horizontal arch permit radius of 7,000 m, while for the value of the permit radius and vertical radius of the vertical arch of 25,000 m. So that the optimization of the horizontal curved radius to 8,502.94 m to be more in line with the ability of the path to serve passing facilities and is expected to be more effective and efficient in planning. The static load and dynamic load of the EMU wheel CR400AF of 81,662.50 N and 243,522.90 N. The maximum voltage and rail clearance voltage were obtained at 134.53 N/mm2 and 228.57 N/mm2. The strength of the rails is written in the form of a safety factor (SF) number. The calculation results show that the most critical SF value of the rail in receiving the load of high-speed trains is 1.70. Based on the results of BoEF calculations, R60 type rails have a high safety value in withstanding static loads and dynamic loads of high-speed trains.

Keywords: *EMU CR400AF, geometry, Railway, High speed, Safety Factor*

INTRODUCTION

A. Rail Road Geometry

The geometry of the rail road is planned based on the planned speed and size of the trains passing through it taking into account factors of safety, comfort, economy, and geographical conditions. Based on the Regulation of the Minister of Transportation Number 7 of 2022 concerning the Implementation of High-Speed Railways, the geometric requirements for high-speed railway roads that must be met include:

1. Horizontal alinyemen

   The horizontal curve planning is shown in Figure 1 As for the following formula: Minimum radius of the curve

   $$R_{min} = 11{,}8 \frac{V^2}{(h_r + h_q)} \quad \text{.....(1)}$$

   Rail elevation planning

   $$V_{max} = \sqrt{\frac{R_r(h_r+h_d)}{11{,}8}} \approx 0{,}29 \sqrt{R_r(h_r + h_d)} \quad \text{..(2)}$$

   $$L_{min\ Transition} \geq \frac{V}{3{,}6} \times \frac{h_r}{f} \quad \text{.....(3)}$$

$h_r = 11{,}8 \frac{V^2}{R} - h_q$ .....(4)

Transition curve planning

$\alpha A - P_1 = \arctan \frac{\Delta x}{\Delta y}$ .....(5)

$\alpha P1 - P_2 = \arctan \frac{\Delta x}{\Delta y}$ .....(6)

$\Delta P_1\text{-}1 = (\alpha P_1 - P_2) - (\alpha A - P_1)$ .....(7)

$d = \sqrt{\Delta x^2 - \Delta y^2}$.....(8)

$\theta_s = \frac{90.L_s}{\pi \times R_{plan}}$ .....(9)

$Lc = \frac{\theta_s}{360} \times 2.\pi.R$ .....(10)

Planning of circular arch components

$X_s = L_s \left(1 - \frac{{L_s}^2}{40 \times {R_{plan}}^2}\right)$ .....(11)

$Y_s = \frac{{L_s}^2}{6 \times R_{plan}}$ .....(12)

$p = \frac{{L_s}^2}{6 \times R_{plan}} - R\,(1 - \cos \theta s)$ .....(13)

$k = L_s - \frac{{L_s}^2}{6 \times R_{plan}} - R\,(1 - \sin \theta s)$ .....(14)

$T_s = (R+p) \times \tan \frac{\Delta s}{2} + k$ .....(15)

$E_s = (R+p) \times \sec \left(\frac{\Delta s}{2}\right) - R_{plan}$ .....(16)

2. Alinyemen vertical

The vertical arch is reviewed by the following parameters:

$A = (g_2\% - g_2\%)$ .....(17)

$L_V = A \times R_V$ .....(18)

$L_{min} = 25$ m.....(19)

$E_V = \frac{A \times L_V}{800}$ .....(20)

$I_p = \frac{g1 - g2}{2} \times R_{sh} + 0{,}4\ V$ .....(21)

3. Superelevation of the arch

Point 1 = $\frac{\frac{1}{4}L_s}{L_s} \times h_r$ .....(22)

Point 2 = $\frac{\frac{1}{2}L_s}{L_s} \times h_r$ .....(23)

Point 3 = $\frac{\frac{3}{4}L_s}{L_s} \times h_r$ .....(24)

Point 4 = $\frac{L_s}{L_s} \times h_r$ .....(25)

where R_{min} is the minimum curvilinear radius, HR is the field plan rail elevation, HQ is the rail elevation deficiency, HD is the rail elevation deficiency boundary, G is the rail road gradient.

The minimum radius of the horizontal curve and vertical curve depend on the speed of the plan, as stated in the following Table 1:

Table 1. The minimum radius of the curve

Plan Speed (km/h)			**350**	**300**	**250**
Minimum radius of	With reply	Normal conditions	7000	5000	3500

horizontal curve (m)		Certain conditions	6000	4500	3000
	Without reply	Normal conditions	7000	5000	3200
		Certain conditions	5500	4000	2800
Minimum radius of vertical curve (m)			25000	25000	20000

B. Dynamic Tools

The axle load of the train which is a static load will turn into a dynamic load when the train is operating. The static load of the train is then multiplied by the dynamic influence factor to obtain the value of the dynamic load of the train. Empirical planning of vertical wheel loads due to dynamic influence factors can be written into equation (25) as follows.

$P = \phi \times Ps$ .....(25)

where P is the plan wheel load, Ps is the static wheel load; and φ is the dynamic influence factor number. The dynamic influence factor number can be determined using various formulas such as AREA, Eisenmann, Talbot, Schramm, etc. One type of dynamic influence factor calculation formula, which uses the equation *The American Railroad Engineering Association* (AREA) in Prause et al. (1972) can be used to determine dynamic influence factors as follows:

$\emptyset = 1+5{,}21\frac{V_R}{D}$.....(26)

where VR is the planned speed (km/h) and D is the mean wheel diameter (mm).

Eisenmann (1972) explained the calculation basis used to determine the dynamic influence factor index with equation (27) as follows:

$\emptyset = 1+\delta.n.t$ .....(27)

where:

$\delta = 0{,}1$ for excellent track conditions

$\delta = 0{,}2$ for good track conditions

$\delta = 0{,}3$ for poor track conditions

$n = 1$ for < speed 60 km/h

$n = 1 + (\frac{V-60}{140})$ for speeds of 60 to 200 km/h

t = 0 to *Upper Confidence Limit (UCL)* 50%

t = 1 to *Upper Confidence Limit (UCL)* 84,1%

t = 2 to *Upper Confidence Limit (UCL)* 97,7%

t = 3 to *Upper Confidence Limit (UCL)* 99,99%

There is a German formula Schramm (1961) used to calculate the dynamic influence index (I_d) with equation (28) as follows:

$I_d = 1 + \frac{4{,}5V^2}{10^5} - \frac{1{,}5V^3}{10^7}$…….....(28)

The Talbot equation (1918) gives the transformation of the dynamic factor multiplier force (I_d) which is described in equation (29) as follows:

$I_d = 1 + 0{,}01\left(\frac{V_R}{1{,}609} - 5\right)$ …….....(29)

C. Rail Maximum Bending Stress

Calculation of the maximum flexural stress of rails using the Beam on Elastic Foundation (BOEF) Analysis method or can also be referred to as beams on elastic foundations, a model used to plan rail road structures. This analysis is used to calculate the bending stress at the base of the rail due to the load of the wheels of the plan train. This modeling was first developed by Winkler (1867) when analyzing rails as continuous beams

on a pedestal of linear elastic foundations. The equilibrium position on an elastic beam receiving a load of q(x) is shown in Figure 1 In the figure, the load distribution q(x) causes the beam to deform so that it moves vertically by y(x) under the axis of the undeformed beam. As a result of the vertical deformai of the beam, a surface contact tension of p(x) occurs.

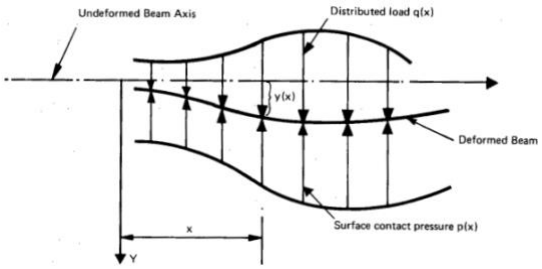

Figure 1. Equilibrum (equilibrium) condition in a deformed beam that receives q(x) loading

The differential equation for the theory of bending in elastic beams as in Figure 1 is written in the following equation.

$EI\frac{d^4y}{dx^4} + ky(x) = q(x)$.....(30)

where y(x) is the vertical deflection at distance x, q(x) is the vertical load distribution, EI is the bending stiffness of the rail, p(x) is the continuous contact stress between bearing and reciprocating and k is the elastic modulus of the rail road.

In equation (30) represents the response of a continuous beam mounted on a spring and receiving a load of q(x) as in Figure 1 In fact, the load of the railway wheel touching the rail is a centralized load, so the load q(x) in equation (30) must be converted into the form of a centralized wheel load P. The solution of deflection, shear force, and bending moment on the rail due to wheel load P is then determined in equation (31), equation (32), and equation (33).

$y_x = \frac{P\beta e^{-\beta x}}{2k}(\cos\beta x + \sin\beta x)$.....(30)

$V_x = \frac{Pe^{-\beta x}}{2}\cos\beta x$ .....(31)

$M_x = \frac{P\beta e^{-\beta x}}{4}(\cos\beta x - \sin\beta x)$.....(32)

$k = \frac{Ps}{Y.S.10^3}$ .....(33)

where y(x) is the deflection of the rail, M_x is the bending moment at the base of the rail, x is the distance to the reference point, P is the vertical load wheel, β is the bending stiffness factor of the beam behaving as an elastic pedestal, and k is the elastic modulus of the rail road.

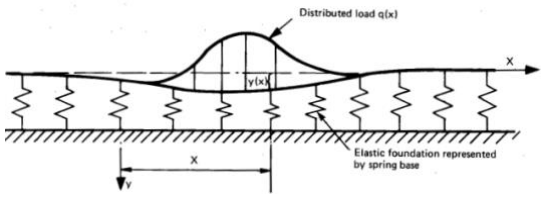

Figure 2. Representation of the load condition q(x) overloading an infinite beam on a continuous pedestal with an elastic foundation base

The modulus value of a rail road can also be determined based on the condition of the rail road (AHLF, 1975) using the following Table 2.

Table 2. Modulus of elasticity of rail road (k) based on rail road conditions

Bearing Condition	Reply Thick (mm)	Reply condition	Subgrade Conditions	k (Mpa)
Bad	150	Relatively noiseless, muddy material	Poor drainage, soft	6,9
Good enough	150	Quite vocal, worthy of mud-free	Medium, moderately drained	13,8
Good	150	Voiced broken stone, mud-free	Medium, moderately drained	20,7
Good	300	Voiced broken stone, mud-free	Medium, moderately drained	27,6
Good	450	Voiced broken stone, mud-free (clean)	Good. Solid, well drained	34,5

D. Rail Clearance Voltage

AREA (1973) suggested that the permit stress value for continuous rails by welding be determined at the base of the rail. (Robnett, et al., 1975). Determination of the strike value of rail permits based on their implications to avoid cracking due to material fatigue. The clearance stress of the rail must be below the value of the melting stress of the material. In other words, the rail clearance stress value is still in the elastic phase of the steel material. The general approach to calculating the clearance flexural stress (σall) proposed by Hay (1953) is given in the following equation (32).

$$\sigma_{all} = \frac{\sigma_y - \sigma_t}{(1+A)(1+B)(1+C)(1+D)} \quad \text{.....(34)}$$

where:

Table 3. Rail clearance voltage reduction factor due to the influence of rail road conditions

Voltage Reduction Factor (Mpa)	There's	Clarke	Magee
Lateral bending influence (A)	15%	15%	20%
Effect of rail road conditions (B)	25%	25%	25% is for branched rail roads, while 35% is for rail road connections
Effects of rail wear and corrosion (C)	10%	10%	15%
Effects of superelevation imbalance (D)	5%	5%	-

E. Rail Safety Factor

Rail safety factor evaluation If the condition is SF>1, the critical condition SF=1 and the failure SF<1.

METHOD

This research was conducted at the office of PT Kereta Cepat Indonesia China located on the Jakarta-Cikampek KM.0+800 Toll Road, Halim Perdana Kusumah, Makassar District, East Jakarta City, Special Capital Region of Jakarta. The research sample was conducted on the Halim road plot until Karawang (KM 0+000 to KM 43+000).

This study seeks primary data in the form of technical specifications of type R60 rails needed to determine the shape, dimensions and quality of steel materials on type R60 rails used in high-speed railway road components, technical specifications of Electric Multiple Unit

CR400AF facilities, as well as vertical and horizontal alinyements of the Jakarta-Bandung Fast Rail section Halim s.d. Karawang to calculate the standard permit geometry of rail roads which will later affect the determination of the operating speed of fast trains.

This study uses quantitative analysis methods including the influence of rail road geometry on train speed with the standards of the Minister of Transportation Regulation Number 7 of 2022, the Beam on Elastic Foundation (BOEF) Analysis method and Chinese Regulation TB 10621 of 2014 concerning the Code for Design of High-Speed Railway.

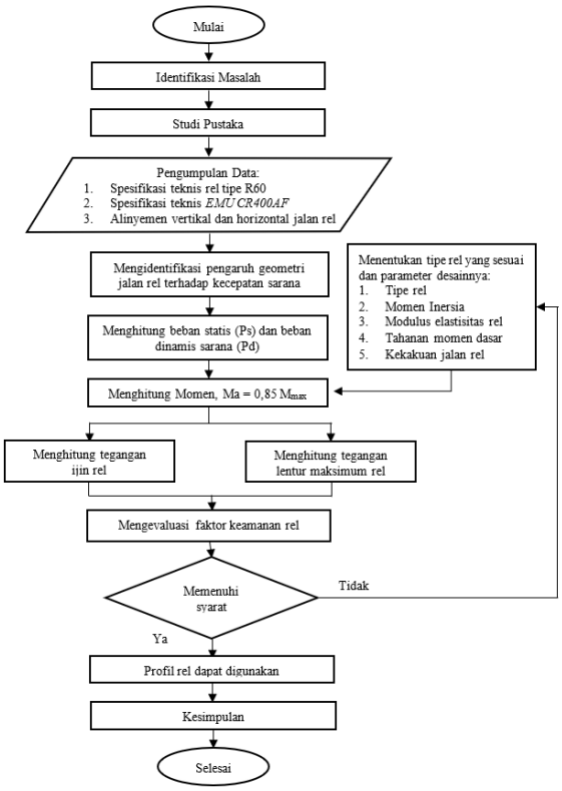

Figure 3. Research method flowchart

RESULTS AND DISCUSSION

A. Rail Road Geometry

1. Horizontal alinyemen

The study was conducted by sampling horizontal curves at locations KM 42 + 410 to KM 44 + 329, with a curved radius of 9500 meters. The maximum speed of the means is planned to be 350 km / h. The width of the rails used is 1435 mm. The horizontal curved data is known as follows.

Table 4. Horizontal alinyemen data

Horizontal Alinyemen Parameters	Result	Unit
V	350,00	km/jam
hr	130,00	mm
hq	40,00	mm
Rmin	8.502,94	m
Vmax Arch	369,00	km/jam
Lmin transition	407,71	m
hrmin	112,16	mm
Rrencana	9.500,00	m

LsPlan		430,00	m
A1	**X**	744.075,31	work
	And	9.297.251,92	work
P1	**X**	747.031,99	work
	And	9.294.486,83	work
A2	**X**	748.449,46	work
	And	9.293.627,51	work
αA-P1		-0,82	work
αP1-P2		-1,03	work
ΔPI-1		-0,21	work
d		4.048,17	m
Ɵs		1,30	degree
Xs		429,98	m
Lc		215,00	m
Ys		3,24	m
p		0,81	m
towards		214,89	m
Ts		771,66	m
Is		3,13	m

The horizontal curvature conditions of the plan can be illustrated in Figure 4 below.

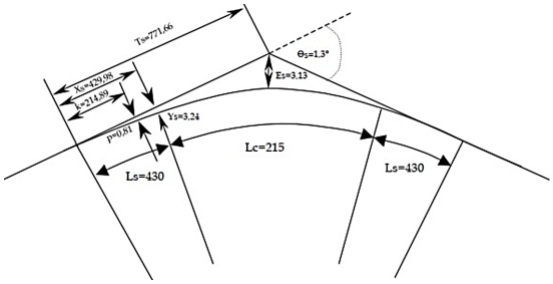

Figure 4. Horizontal curved illustration

A minimum radius of horizontal curve of 8,502.94 m is obtained ⩽ Realized = 9500 m. So that the design of the horizontal alignment can be optimized in its horizontal curved radius to 8,502.94 m to be more in line with the ability of the path to serve passing facilities and is expected to be more effective and efficient in planning. The results of the horizontal curve evaluation can be seen in Figure 5, it is known that the green line is the realization horizontal curve, while the red line is the result of the horizontal curve evaluation.

Figure 5. Horizontal arch evaluation KM 42+410

2. Alinyemen vertical

The study conducted vertical arch sampling at locations KM 42 + 332 to KM 43 + 955 with a vertical curve radius of 25000 meters.

Table 6. Vertical infrastructure data

Radius (m)	Start (km)	End (km)	Curvilinear Length(m)	Full Arch (m)	Initial Gradient, g1 (%)	Final Gradient, g2 (%)
25000	42+332,68	43+955,06	1662,38	349,935	0,6	2,0

The evaluation of the vertical curve is reviewed by several parameters by referring to equation (17) to equation (21) as follows:

Table 7. Vertical curve calculation result

Vertical Alignment Parameters	Result	Unit
Curvilinear Location	KM 42+332 s.d KM 43+955	
Rv	25000	m
Vplan	350	km/jam
g1	0,600	%
g2	2,000	%
A	1,40	m
Lv	35000	m
Home	61,250	m
Lp	17640	m

The vertical curvilinear conditions of the plan can be illustrated in Figure 6 below.

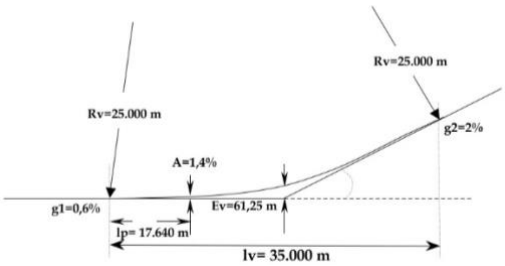

Figure 6. Vertical curved illustration

The results of further analysis by referring to the vertical curve radius requirements in Table 1 that the minimum radius of the vertical arch is 25,000 m while the radius of realization of the vertical arch is 25,000 m. So that the vertical alignment has met the vertical alignment requirements based on the Minister of Transportation Regulation Number 7 of 2022.

3. Superelevation of the arch

The planning of the superelevation of the arch continues from the calculation data in Table 5 which is known the value of hrmin is 112.16 mm, Lc is 215 m and Ls is 430

m. Then this study calculated the design of curved superelevation by referring to equation (22) to equation (25) with the following results.

Table 8. Results of curvilinear superelevation calculation

Curved Superelevation Parameters	Result	Unit
LsPlan	430,00	m
Lc	215,00	m
hr	112,16	mm
-Point 1	28,04	mm
-Point 2	56,08	mm
-Point 3	84,12	mm
-Point 4	112,16	mm

The condition of the planned arch superelevation can be seen in 7 where the arch superelevation is carried out on the outer rail of the transition arch section by dividing it into 4 elevation points that have varying heights, namely 28.04 mm, 56.08 mm, 84.12 mm, and 112.16 mm.

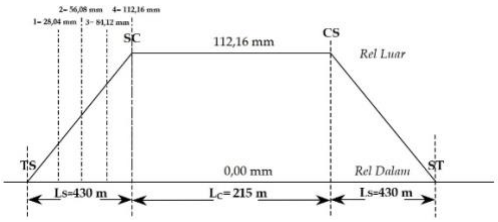

Figure 7. Illustration of curved superelevation

B. Dynamic Load Means

The axle load of the train used in this study used the train load of series number 6 or TP 06 weighing 65.3 tons. In the calculation of rail strength against vertical loading of high-speed trains, the use rests on a load of 1 wheel (PS), so that the weight of the means wheels is 81,662.50 N, and the maximum speed of the EMU CR400AF means is 350 km / h, with wheel dimensions of 920 mm. This study compares several references to dynamic influence factors from several countries such as America and Germany, namely AREA (1972), Eisenmann (1972), Schramm (1961) and Talbot (1918) which refer to equations (26) to equations (29) with the following calculations.

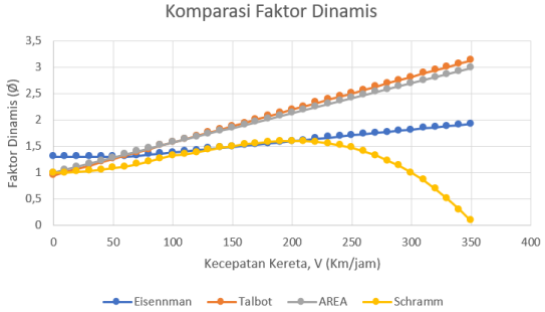

Figure 8. Dynamic influence factor comparison

The relationship of dynamic influence on train speed is shown in Figure 8. In the figure displayed the dynamic influence factor when the maximum speed of the means is 350 km / h according to Eisenmann, Talbot, AREA, and Schramm theory of 1.92, 3.13, 2.98, and 0.08 respectively. The four graphs of the relationship of speed with dynamic influence factors show values that are directly proportional to each other. Schramm's (1961) graph shows the value of a dynamic influence factor that begins to decrease at speeds exceeding 200 km / h. Talbot's (1918) and AREA's (1974) graphs show the value of the increase in dynamic factor directly proportional to each increase in speed, and this study considers the value of the dynamic factor to be the most applicable because the value is close to the provisions in the Chinese regulation TB 10621 which requires a dynamic factor value of 3.0. Therefore, this study uses the calculation of dynamic influence factors of AREA theory (1974) by referring to equation (26) and obtained the following values.

$Ø = 1+5{,}21 \text{ x } \frac{V_{maks}}{D} = 1 + 5{,}21 \text{ x } \frac{350}{920} = 2{,}98$

So that the dynamic load of 1 wheel means as follows:

$P_d = Ø \text{ x } P_s = 2{,}98 \text{ x } 81.662{,}5 = 243.552{,}90 \text{ N}$

C. Rail Maximum Voltage

The rail technical indicators used in the Beam on Elastic Foundation (BoEF) analysis include dimensions, melting stress, modulus of elasticity, melting stress of rails, moment of inertia, static moment modulus of rail roads. The melting stress value of rail steel type R60 is required, which is 1040 Mpa. Thus, the license stress analysis of rail steel in this study is determined under the ultimate limit conditions. The rail technical indicator data are shown in Table 9 as follows.

Table 9. Technical indicators of rail type R60

Parameter	Value	Unit
Massa Rail (w)	60	kg/m
Cross-sectional area	77,45	cm2
Distance from center of gravity to the bottom of the rail	8,12	cm
distance from center of gravity to the head of the rail	9,48	cm
Moment of inertia to the horizontal axis (Ix)	3.217,00	cm4
Moment of inertia to the vertical axis (Iy)	524,00	cm4
Statis momen	396,18	cm3
Modulus of elasticity of rails (E)	200.000	N/mm2
Bearing Distance(s)	0,60	m
rail density	7.800,00	kg/m3
Rail melting stress	1040,00	N/mm2
Track modulus of elasticity	27,60	N/mm2

In such a condition, that the axle load of the means imposed on the rail road structure is not only affected by one axle but also influenced by the position of other adjacent axles is referred to as axle superposition. The axle clearance condition of the EMU cabin cars can CR400AF be seen in Figure 9 below.

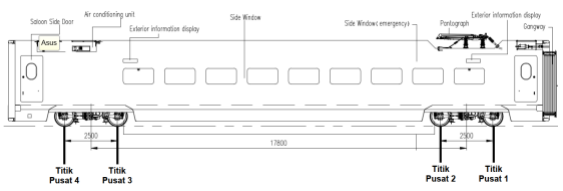

Figure 9. EMU CR400AF Dimensions

Calculation of the maximum bending moment moment at the wheel load point (M_{max}) with equations (30) to equations (33). The maximum bending stress of the rail occurs on the rail located directly under the wheel. The most critical bending moment resulting from the combination of bending moments due to wheels close to each other is 5.33 t.m. So the value of the stress on the rail must be calculated by the following equation.

$$\sigma_b = \frac{M_{max}}{Z_x} = \frac{5{,}33\ x\ 10^7}{396.182{,}27} = 134{,}53\ \text{N/mm}^2$$

D. Rail Clearance Voltage

The analysis of permit flexural stress (σ_{ijin}) in this study assumes that some stress due to changes in weather temperature are ignored and rail clearance stress reduction due to the influence of field conditions using the values proposed by Hay and Clarke referred to in Table 3, namely A = 15%, B = 25%, C = 10%, and D = 5%. The rail clearance voltage is determined using equation (34) as follows:

$$\sigma_{all} = \frac{\sigma_y - \sigma_t}{(1+A)+(1+B)+(1+C)+(1+D)}$$

$$= \frac{1040}{(1+15\%)+(1+25\%)+(1+10\%)+(1+5\%)}$$

$$= 228{,}57\ \text{N/mm}^2$$

The results of the calculation above show that the maximum rail pressure value at the bottom of the rail is σb = 1.70 ≤ σijin = 228.57 N/mm, so that the Type R60 rail can be concluded to be safe in withstanding the maximum pressure of train wheels number 6 or *TP06 EMU CR400AF* that cross it.

E. Safety Factor (SF) Rail

Calculation of rail safety factors with the following formula:

$$SF = \frac{\sigma_{all}}{\sigma_x}$$

$$= \frac{228{,}57}{134{,}53} = 1{,}70 \geq SF_{permit} = 1{,}00 \text{ (secure)}$$

The most critical safety factor (SF) number due to the load of train series number 6 or TP06, all safety factor (SF) values of rails due to the most critical facility load in Table 10, shows that all SFactual values = 1.70 > SFlicense = 1, so that Type R60 rails can be concluded to be safe in bearing the load of train number 6 *EMU CR400AF* that crosses it. The SF value describes the level of confidence of an *engineer* to plan the structure to ensure the strength of the rail structure in bearing the load. Until the time this study was written, this study had not found a recommended reference ideal SF value to guarantee the safety of rail structures calculated by the method *Beam on Elastic Foundation.*

Table 10. Rail Safety Factor Evaluation

Location	Distance (mm)	bending moment, Mx (t.m)	Bending Voltage, σx (N/mm2)	Allowable voltage, σall (N/mm2)	Safety Factor (SF)	Cheque
Center 1	0	5,33	134,53	228,57	1,70	Secure
Center 2	2.500	5,33	134,53	228,57	1,70	Secure
Center 3	15.300	5,33	134,53	228,57	1,70	Secure
Center 4	17.800	5,33	134,53	228,57	1,70	Secure

F. Analysis Recapitulation

The results of the recapitulation of the analysis of the geometry of rail roads and the strength of rails against the loading of high-speed trains are shown in Table 11 by referring to the technical requirements of rail roads in Table 1 as follows:

Table 11. Recapitulation of Analysis of Rail Road Geometry and Rail Strength Against High-Speed Train Loading

No	Account	Unit	Allowed values	The value of the calculation result	Information
1	Horizontal Curved Radius				
	Realization Radius	m	≥ 7.000,00	9.500,00	Secure
	Radius minimal	m	≥ 7.000,00	8.502,94	Secure
2	Vertical Curved Radius	m	25.000,00	25.000,00	Secure
3	Rail Maximum Bending Stress (σx)	N/mm	≤ 228,57	134,53	Secure
4	Rail Safety Factor (SF)	-	≥ 1,00	1,70	Secure

From the table above it can be seen that:

a. The realization radius and minimum radius of the horizontal arch are 9500 m and 8502.94 m respectively ⩾ The permit radius of the horizontal arch is 7000 m. So that the horizontal alignment has met the requirements of the horizontal instrument. Then optimization was carried out on the radius of the horizontal curve to 8,502.94 m to be more in line with the ability of the path to serve passing facilities and is expected to be more effective and efficient in planning;
b. The radius of the vertical arch permit is 25,000 m while the radius of realization of the vertical arch is 25,000 m. So that the vertical alignment has met the requirements of the vertical instrument;
c. The maximum rail pressure at the bottom of the rail is σ b = 134.53 ⩽ σ ijin = 228.57 N/mm, so that the Type R60 rail can be concluded to be safe in withstanding the maximum pressure of train wheels number 6 or TP06 EMU CR400AF crossing it; and
d. The actual rail safety factor (SF) is 1.70 > SFijin = 1, so that Type R60 rail can be concluded to be safe in bearing the weight of train wheel number 6 or TP06 EMU CR400AF that crosses it.

CONCLUSION

Based on the results of the analysis that has been carried out, it can be concluded that several things, namely the horizontal and vertical infrastructure of the Jakarta-Bandung high-speed train line at KM 42+840 have a planned radius of 9500 m and 25000 m taking into account the maximum train speed of 350 km / hour. The minimum radius values for horizontal and vertical instruments on trains traveling at speeds of 350 km / h are 8,502.94 m and 25000 m. Optimization of the horizontal curved radius to 8,502.94 m to be more in line with the ability of the line to serve passing facilities and is expected to be more effective and efficient in

planning. The dynamic influence factor of the American Railroad Engineering Association (AREA) shows a value of 2.98. The increase in dynamic factor is directly proportional to each increase in speed and is most applicable compared to other dynamic factors such as Schramm, Eisennman and Talbot because the value is close to the provisions in the Chinese regulation TB 10621 which requires a dynamic factor value of 3.0. So that the static load and dynamic load of the EMU cabin cars wheels CR400AF 81,662.50 N and 243,522.90 N. The most critical bending moment is the result of a combination of bending moments due to wheels that are close to each other which is 5.33 t.m. So that the maximum bending stress of the rail occurs on the rail located just below the wheel, which is 134.53 N/mm. The flexural voltage of the R60 type permit uses the Hay equation which is 228.57 N/mm, and the Safety Factor (SF) of the R60 type rail due to the loading of train number 6 or TP06 EMU CR400AF which is 1.70. SFreal value = 1.70 ≥ SFijin = 1 thus the rail is declared safe in receiving the EMU wheel load CR400AF.

Some suggestions that can be done for further research, among others, until now, this study has not found the recommended safety factor (SF) value to ensure the safety of rail structures so that in the Minister of Transportation Regulation or PT KCIC Company Regulation to provide a basis for calculating rail loading on facilities to provide guidance in calculating rail strength. Further research can analyze rail strength by adding longitudinal and lateral load variables due to crossing facilities. And for further research that is more thorough, it can add the basis for calculating the elastic modulus of rail roads (tracks) on ballasted and ballastless lines.

REFERENCES

Adi, W. T. (2019). Kajian Umur Jalan Rel Berdasarkan Keausan dengan Metode dari AREA dan Perjana. *Jurnal Perkeretaapian Indonesia (Indonesian Railway Journal)*, *3*(2). https://doi.org/10.37367/jpi.v3i2.84

Aghastya, A., Wardana, A., Tamtomo Adi, W., Ahda Imron, N., & Artha Wirawan, W. (2023). Geometry Design of Railway Track for High-Speed Railways Bandung-Cirebon KM 00+000 - KM 33+850. Journal of Railway Transportation and Technology, 2(2), 34–45. https://doi.org/10.37367/jrtt.v2i2 .29

Ashadi, R. F., Citra, Z., Sari, I. P., Sipil, T., Buana, U. M., & Barat, J. (2023). Penilaian Risiko Proyek Infrastruktur Kereta Api Cepat Jakarta – Bandung. *Journal Of Civil Engineering and Vocational Education*, *10*(2), 564–577. https://ejournal.unp.ac.id/index.php/cived/article/download/122678/108074

CRRC Qingdaio Sifang Co., L. (2020). *Technical Specification Jakarta Bandung High-Speed EMU*.

Doyle, N. (1980). *Railway Track Design. A Review Of Current Practice*. BHP Melbourne Research Laboratories.

Esveld, C. (2001). *Modern Railway Track Second Edition. Delft University of Technology*. Delft University of Technology.

Fajriati, R., Mada, U. G., Muthohar, I., Mada, U. G., Hapsoro, S., Utomo, T., Mada, U. G., Suparma, L. B., & Mada, U. G. (2020). Analisis Risiko Derailment Pada Kereta Api. *Prosiding Forum Studi*, 23–24.https://ojs.fstpt.info/index.php/ProsFSTPT/article/download/651/601

Isradi, M., Dwiatmoko, H., Setiawan, M. I., & Supriyatno, D. (2020). Analysis of Capacity, Speed, and Degree of Saturation of Intersections and Roads. *Journal of Applied Science, Engineering, Technology, and Education*, *2*(2), 150–

164.https://doi.org/10.35877/454ri.asci22110

Kementerian Perhubungan. (2012). *Peraturan Menteri Perhubungan No. 60 Tahun 2012 Tentang Persyaratan Teknis Jalur Kereta Api* (pp. 1–57). Kementerian Perhubungan Republik Indonesia.

Kementerian Perhubungan. (2022). *Peraturan Menteri Perhubungan No. 7 Tahun 2022 Tentang Penyelenggaraan Kereta Api Kecepatan Tinggi* (pp. 208–227). Kementerian Perhubungan Republik Indonesia.

Lu, C. F. (2019). A discussion on technologies for improving the operational speed of high-speed railway networks. Transportation Safety and Environment, 1(1), 22–36. https://doi.org/10.1093/tse/tdz003

Mardia, N., & Widyaningsih, N. (2019). Analisis Kinerja Simpang Bersinyal Dan Ruas Jalan (Studi Kasus: Simpang Dan Ruas Jl. Panjang Yang Terhubung Dengan Jl. Kedoya Duri Dan Jl. Duri Raya). *Jurnal Kajian Teknik Sipil*, *4*(2), 154–164. https://doi.org/10.52447/jkts. v4i2.1539

Prativi, A., & Adi, W. T. (2020). Evaluasi Kekuatan Rel UIC54 Menggunakan Metode Beam On Elastic Foundation (BOEF). *Jurnal Perkeretaapian Indonesia (Indonesian Railway Journal)*, *4*(2),117–123. https://doi.org/10.37367/ jpi.v4i2.101

Rizqi Fitriansyah, E., & Putri Elza, S. (2023). Kajian Shear Lag Pada Sambungan Tarik Baja Profil WF Dengan Metode Elemen Hingga. *Jurnal Teknik Sipil*, *12*(1), 1–8. https://jurnal.usk.ac.id/JTS/index

Rosyidi, S. A. P. (2016). *Rekayasa Jalan Kereta API Tinjauan Struktur Jalan Rel* (Cetakan II). LP3M UMY.

Van Dyk, B. J., Edwards, J. R., Dersch, M. S., Ruppert, C. J., & Barkan, C. P. L. (2017). Evaluation Of Dynamic And Impact Wheel Load Factors And Their Application In Design Processes. *Proceedings of the Institution of Mechanical Engineers, Part F: Journal of Rail and Rapid Transit*, *231*(1), 33–43. https://doi.org/10.1177/0954409715619454

Yudistirani, S. A., Diniardi, E., Basri, H., & Ramadhan, A. I. (2021). Analisa Keausan Dan Faktor Keamanan Keluar Rel Pada Kereta Api Lokomotif. *Jurnal Teknologi*, *13* (2), 209–216. https://jurnal.umj.ac.id/index.php/jurtek/article/view/9960

Yusuf, M. A., Roestaman, R., & Walujodjati, E. (2022). Evaluasi Struktur Atas Komponen Jalan Rel dalam Kegiatan Reaktivasi Jalur Cibatu Cikajang. *Jurnal Konstruksi*, *20*(1), 30–40. https://doi.org/ 10.33364/konstruksi/v.20-1.926